

A Roadmap for enhancement of Global Geodetic Reference Frame

*Basara Miyahara¹

1.GSI of Japan

The United Nations General Assembly adopted its resolution, "Global Geodetic Reference Frame for Sustainable Development", on February 26, 2015, recognizing that Global Geodetic Reference Frame (GGRF) is essential fundamental infrastructure for social, economic and scientific activities. This resolution is the first resolution on the importance of a globally-coordinated approach to geodesy and urges Member States to jointly develop and maintain sustainable GGRF under globally-coordinated multilateral cooperation. The resolution includes six Operational Paragraphs which urge Member States to establish a Roadmap for the enhancement of GGRF, enhance technical assistance and capacity building on geodesy, and maintain and improve their geodetic infrastructure and so on. The resolution was first drafted by Working Group of geodetic experts which was established by UNCE-GGIM and adopted by the committee at its forth session. The United Nations Economic and Social Council then adopted the resolution and finally it was table to the UN General Assembly by Fiji co-sponsored by 52 Member States including Japan. Geospatial Information Authority of Japan (GSI) has participated in the Working Group form the beginning and contributed to the development of the draft resolution. GSI has also participated in development of the GGRF Roadmap. In the roadmap, the Working Group clarifies current issuers for maintenance of sustainable GGRF, then suggests the possible solutions and finally presents future vision for the further enhancement of GGRF. The roadmap will be reported to UNCE-GGIM at its sixth session in New York on August 2016. In this presentation, I will review the background and the purpose of the resolution and report the overview of the Roadmap which promotes the enhancement of GGRF.

Keywords: global geodetic reference frame, the United Nations General Assembly resolution, Global Geodetic Observing System

Status Report on the Ishioka Geodetic Observing Station

*Takahiro Wakasugi¹, Masayoshi Ishimoto¹, Ryoji Kawabata¹, Yoshihiro Fukuzaki¹, Kojin Wada¹

1.GSI of Japan

The Geospatial Information Authority of Japan (GSI) has constructed a new geodetic observing station including an up-to-date VLBI radio telescope in Ishioka City, Ibaraki Prefecture. Besides the VLBI radio telescope and GNSS CORSS that were already completed in March 2014, Absolute Gravity points will be available after completion of the observing building in February 2016. We will report the recent status of the whole facilities in Ishioka station. In addition, we will also mention the preliminary results of VLBI experiences carried out using the new radio telescope.

Satellite laser ranging network: Where should a new station be placed?

*Toshimichi Otsubo¹, Koji Matsuo², Keiko Yamamoto³, Yuichi Aoyama⁴, Thomas Hobiger⁵, Mamoru Sekido⁶, Toshihiro Kubooka⁶

1.Hitotsubashi University, 2.Geospatial Information Authority of Japan, 3.Japan Aerospace Exploration Agency, 4.National Institute of Polar Research, 5.Chalmers University of Technology, 6.National Institute of Information and Communications Technology

About 40 stations are being operational all over the world for satellite laser ranging but the distribution of the current station network is not uniform. To enhance the accuracy of the terrestrial reference frame promoted by the IAG's component GGOS, a simulation analysis is conducted assuming a new station is added to the existing network. A simulation data set for the new station is created based on the actual data yield statistics of the existing stations. Six geodetic satellites, LAGEOS-1, -2, Ajisai, LARES, Starlette and Stella are used in this study. The space geodesy analysis software 'c5++' is run, in its simulation mode, with and without the new station, and the difference of the estimated error for each parameter is examined. It is found that the network gaps especially in the southern hemisphere should be filled and also that the best position depends on a target geodetic parameter. For instance, a high latitude station performs best for the X and Y components of the geocenter but a low latitude station performs best for the Z component.

Keywords: Space Geodesy, GGOS, Satellite Laser Ranging, Precise Orbit Determination, Terrestrial Reference Frame, Gravity

Orbital perturbation of geodetic satellites detected by the time variation of empirical acceleration

*Akihisa Hattori¹, Toshimichi Otsubo²

1.Hitotsubashi University, Faculty of Social Sciences, 2.Hitotsubashi University

State-of-the-art satellite laser ranging systems have reached the precision better than 1 cm. Precise orbit determination using satellite laser ranging data should fully utilize such a high precision. However, each dynamic model is not accurate enough and there are still unsolved questions.

Quality of dynamic models directly impacts that of orbit determination. Empirical acceleration expressed as simple functions is generally introduced so that the parameters absorb unmodeled forces and reduce the residuals (Otsubo et al 2014).

The purpose of this study is to extract unknown acceleration factors from systematic behavior of empirical parameters and provide geodetic or geophysical explanations. Thermal acceleration models were discovered over the analysis of the empirical acceleration (Scharoo et al 1991).

"c5++" is space geodetic analysis software developed by Hitotsubashi University, NICT and Chalmers University of Technology. This software can estimate empirical acceleration constant terms and periodic terms in along-track, cross-track and radial components.

We use "c5++" to estimate empirical acceleration parameters of six geodetic satellites: AJISAI, LAGEOS-1, LAGEOS-2, LARES, STELLA and STARLETTE for the past five years. Five empirical parameters are estimated per arc. One is a constant term in the along-track component, two are periodic terms in the along-track component and the rest two are periodic terms in the cross-track component. The post-fit residual RMS is 7-10 mm for LAGEOS-1 and LAGEOS-2 and 20-40 mm for the other low-orbit satellites.

In the LAGEOS-1 and LAGEOS-2 cases, the magnitude of the along-track constant term is 0-10 pm/s², that of the along-track periodic terms is 0-200 pm/s², and that of the cross-track periodic terms is 0-1 nm/s². In the low-orbit satellite cases, these values are 0-2 nm/s², 0-2 nm/s² and 0-10 nm/s², respectively.

A frequency analysis is applied to the five-year time series of empirical acceleration parameters. For example, the periodic terms of the along-track component of AJISAI are found to have high correlation with the absolute value of the angle between the satellite orbital plane and the Sun. Analyzing such systematic time variations of empirical acceleration parameters should help to extract unknown phenomena in satellite dynamics.

Keywords: satellite laser ranging; SLR, empirical acceleration

Improvement of an Estimation Method of GEONET Fixed Point Coordinates

*Yuki Kamakari¹, Hiromi Yamao¹, Yuki Hatanaka¹

1.GSI of Japan

The Geospatial Information Authority of Japan (GSI) is processing the daily GEONET station data with GEONET analysis strategy called F3, which is based on ITRF2005. The daily coordinates of all GEONET stations are calculated in this analysis and the results are used for a variety of purposes such as the monitoring of crustal movements around Japan.

In the F3 analysis, a GEONET station "TSUKUBA1" is used as a fixed point for the calculation of the daily coordinates of all GEONET stations. The coordinate of "TSUKUBA1" is estimated from IGS stations around Japan, whose a priori coordinates are given using the ITRF2005 coordinate/velocity set.

Previously, the number of IGS stations used in the coordinate estimation of TSUKUBA1 were around twenty. But today, the number has decreased almost by 40%, since the IGS stations replaced or affected by Tohoku earthquake are removed from the estimation.

As a result, the estimated coordinate value became vulnerable to data outages of the IGS stations. In order to reduce negative effect of data outages on the resulting coordinate value, we reselected the IGS stations used in the coordinate estimation of TSUKUBA1. Using the reselected 20 IGS stations, we evaluated the stability of the coordinate of Tsukuba1 and verified that sufficient stability is achieved.

Keywords: GEONET, GNSS

Green function for internal deformation due to a point dislocation in a spherical earth: asymptotic solution at the higher degree for a stratified earth model

*Yu Takagi¹, Shuhei Okubo²

1.School of Science, The University of Tokyo, 2.Earthquake Research Institute, The University of Tokyo

Green functions representing the deformations (e.g. displacement and strain) due to a point mass load and point dislocations play important roles in geodesy and seismology. For example, the 'surface' Green function for a mass load (Farrell, 1972) has been used to calculate gravity and strain changes caused by ocean tides. The 'surface' Green function for point dislocations (Sun & Okubo, 1993) is necessary to interpret displacement and gravity changes caused by great earthquakes. The 'internal' Green function for point dislocations will enable us to estimate stress changes such as Coulomb's static stress changes excited by great earthquakes. The asymptotic solution representing the behaviour of the solution at higher degree ($n \rightarrow \infty$) is useful because the solution at higher degree up to several thousands or tens of thousands are needed to obtain these Green functions. The asymptotic solutions for 'surface' deformation due to a point mass load and point dislocations were found by Farrell (1972) and Okubo (1988), respectively. However, asymptotic solution for 'internal' deformation due to point dislocations has not been obtained yet except for that of homogeneous sphere (Okubo & Takagi, 2014 JpGU). We need it for a stratified earth model. In case of a spherically symmetric earth model with self-gravitation, deformation fields are divided into the spherical and toroidal fields and they are represented as 6th and 2nd order differential equations. We assume that 'the solution for a stratified earth' = '(i) the solution for a homogeneous sphere' + '(ii) the effect of radial variance of the structure'. The effect (ii) is calculated by using the solution for a homogeneous sphere (i) that has already been obtained (Okubo & Takagi, 2014 JpGU). Although the effect (ii) is represented by an integral over the whole earth volume, we have only to consider the effect around the depth of the source and the depth where the deformation is evaluated at the higher degree.

We calculated the asymptotic solution for the toroidal field following the above idea and presented it in an analytical expression. We verified that the analytical expression agrees to numerical solution in an asymptotic sense when the degree n becomes large (over 10,000) as expected. In this presentation, we will show the asymptotic solution for the spheroidal field in addition to that for the toroidal mode, and discuss the usefulness of it.

Keywords: Green function, point dislocation, internal deformation, stratified earth, asymptotic solution

Evaluation of the error propagation in GPS/A measurement using a moored buoy

*Misae Imano¹, Motoyuki Kido^{1,2}, Yusaku Ohta¹, Narumi Takahashi^{3,4}, Tatsuya Fukuda⁴, Hiroshi Ochi⁴, Ryota Hino¹

1.Reserch Center for Prediction of Earthquakes and Volcanic Eruptions Graduate School of Science, Tohoku University, 2.International Research Institute for Disaster Science, 3.National Research Institute for Earth Science and Disaster Prevention, 4.Japan Agency for Marine-Earth Science and Technology

Tohoku University, Japan Agency for Marine Earth Science and Technology (JAMSTEC), and Japan Aerospace Exploration Agency (JAXA) have co-developed a continuous observation system for horizontal and vertical crustal deformation and tsunami using a moored buoy (Takahashi et al., 2014). The third sea-trial has been carried out in the supposed source region near the Nankai Trough. A seafloor transponder array is installed on the depth of 3 km which consists of six transponders forming a ~3 km-wide triangle. The target accuracy in horizontal positioning of this system is on the order of 1 m to detect the seafloor deformation associated with a M8-class earthquake.

The buoy in the system (1) has difficulty to keep a fixed point and (2) is often located along the circumference of 4 km-radius due to the mooring cable is longer than the water depth by 1.5 times. These factors are thought to have an influence to the array positioning as (1) the systematic error due to an error in array geometry (relative positions of individual seafloor transponders) and (2) the larger error than those near the array center. However, the error propagation in the buoy system has not been ever clarified quantitatively. Therefore, we examined the error propagation in GPS/A measurement using a moored buoy through numerical experiments. Then we proposed how to improve the accuracy of the system based on the result of the experiments.

Possible error sources in the buoy system are a vertical buoy position error in kinematic Precise Point Positioning (PPP, Zumberge et al., 1999), an attitude error, which is equivalent to a horizontal buoy position error, traveltime error, and array geometry error. We estimated the array position with the above error and synthetic data on the grid in 10 km square every 100 m. We assumed the errors as following.

1. A vertical buoy position error in post processing kinematic PPP: normal distribution (1 σ : 4 cm, Ohta et al., 2006)
2. Travel time error (false picking by 1 peak and picking resolution): uniform distribution (± 0.1 ms) and normal distribution (± 0.01 ms).
3. Array geometry error: normal distribution (1 σ : horizontal 15 cm, vertical 25 cm)

The largest errors in array positioning amount to 1. 10-20 cm, 2. 30-40 cm and 3. 50--150 cm for each error source. Amount of the propagated error is linearly proportional to the error sources. The numerical experimental results generally agree with the array position error in the second trial. Array geometry error is found to be most significant. The array geometry must be determined with a few cm-accuracy to achieve the final positioning accuracy on the order of 1 m in the future. Acknowledgements: This study was supported by the MEXT through the Project for Development of GPS/Acoustic Technique and by JST Cross-ministerial Strategic Innovation Promotion Program (SIP, Reinforcement of resilient function for preventing and mitigating disasters).

Keywords: Seafloor crustal deformation, A moored buoy, GPS/Acoustic measurement

Monitoring of moored buoy attitude by single GPS antenna and rate-gyro

*Chie Honsho¹, Motoyuki Kido¹, Yusaku Ohta², Misae Imano²

1.International Research Institute of Disaster Science, Tohoku University, 2.Graduate School of Science, Tohoku University

Tohoku University, Japan Agency for Marine-Earth Science and Technology (JAMSTEC), and Japan Aerospace Exploration Agency (JAXA) has developed real-time observation system for tsunami and crustal movement using a moored buoy in the SIP (Cross-Ministerial Strategic Innovation Promotion Program) "Reinforcement of resilient function for preventing and mitigating disasters". The Tohoku University team is in charge of the GPS/Acoustic seafloor positioning. The current buoy system is equipped with four GPS antennas formed into a 1 m x1 m square on the top, which compose a GPS gyro system and provide buoy attitude as well as position of the main antenna. The four GPS antenna system has much less power consumption (~6 W) compared with fiber optic gyro or ring laser gyro, but further power saving system is desirable for observation of long duration. We propose a method to monitor buoy attitude using one GPS antenna and a MEMS 3-axis gyroscope/accelerometer (<1 W power consumption). We analyzed data collected during a sea trial to examine accuracy of attitude obtained from the single-antenna system.

There are two observation equation describing (1) the relationship between 3-axis angular rate and the rate of change of attitude angles (yaw, pitch, and roll), and (2) that amount of change of GPS antenna velocity equals to the sum of integral value of acceleration and amount of change of velocity by rotation. The time variation of yaw, pitch, and roll was each expanded in cubic B-spline basis functions, and the expansion coefficients were calculated using the method of nonlinear least squares. We utilized angular rate and acceleration data (10 Hz) measured by a MEMS gyro (Xsens, MTi-G) and time differential values of GPS antenna position data (1 Hz) obtained by kinematic PPP analysis for antenna velocity. During a sea trial conducted off Kii Peninsula in 2014, observations ~20 minutes long were repeated once a week for four months, and we chose data of 8 observations 19 minutes long without missing data. Besides, we performed the estimation of true buoy attitude variation using GPS gyro data (JAVAD, Sigma-Q) for the comparison with the results from the single-antenna system. Instead of interpolating GPS gyro data, attitude variations were estimated considering errors in GPS gyro data by using together rate data provided by MEMS gyro. The error of GPS gyro data was estimated as 0.2 °, almost equivalent to the nominal accuracy, and that of MEMS rate data as 0.6 °/s, twice the nominal accuracy.

Errors of attitude angles obtained from our method were 0.5 °, 1.3 °, and 1.0 ° for yaw, pitch, and roll, respectively. These amounts correspond to the horizontal and vertical position errors of transducer of 9 and 3 cm, respectively. Although the accuracy is not enough at present, it was shown that a small rotation of the axes of MEMS gyro relative to those of GPS gyro, which results in bias errors, caused considerable part of the errors. Errors actually have common bias among all observations, and amount of the rotation was estimated as -0.1 °, -1.3 °, and -1.0 ° for yaw, pitch, and roll, respectively. Errors still remaining after correction for the rotation arise from the limited ability of the method including accuracy of data. The errors were 0.5 ° for yaw and 0.4 ° for pitch and roll. It was confirmed by trail measurements on board a research vessel that errors in pitch and roll could be reduced to as small as 0.03 ° when using a high-performance MEMS gyro with higher accuracy (Xsens, MTi-G700). Considering that error of yaw angle less affects final result of acoustic ranging than that of pitch and roll, yaw with 0.5 ° error is practically sufficient. Therefore, we conclude that the single-antenna system can provide attitude with enough accuracy. However, rotation of the MEMS gyro coordinates relative to the buoy coordinates directly results in

attitude errors. The task is to establish technique to fix the rotation angles.

Keywords: GPS/Acoustic seafloor positioning, MEMS gyroscope/accelerometer

Detecting localized seafloor deformation using traveltime difference of acoustic signals of transponders nearby --Observation in the Japan Trench--

*Motoyuki Kido¹, Juichiro Ashi², Takeshi Tsuji³, Fumiaki Tomita⁴

1.International Research Institute for Disaster Science, Tohoku University, 2.Atmosphere and Ocean Research Institute, University of Tokyo, 3.International Institute for Carbon-Neutral Energy Research, 4.Graduate School of Science, Tohoku University

There often found fault-like feature near axis seafloor in the subduction zones, which may be formed through repeating occurrence of earthquake cycle. It is almost unrevealed when these faults are activated in the cycle because of the lack of in-situ geodetic measurement. Direct-path seafloor ranging technique is known to be suitable for monitoring the activity of such a fault. However, this technique sometimes has a difficulty to keep clearance along the acoustic path due to topographic obstacle. Here we proposed a modified GPS/Acoustic technique that intrinsically needs no direct-path and can precisely measure relative motion of two seafloor transponders lied along a short baseline. We applied this new technique at a cliff in the Japan Trench, which is interpreted as a backthrust.

Accuracy of direct-path seafloor ranging tends to be proportional to the baseline length, say 1 cm/km, for instance. While the accuracy of individual positioning of transponder in GPS/A measurement is a few to several tens of cm. This is mainly due to spatio-temporal variation of sound speed, kinematic GPS analysis, traveltime detection in acoustic waveforms. If a pair of seafloor transponders is installed across a fault, traveltime difference can be precisely determined because of similarity of the waveform. In addition, effect of the sound speed variation is almost cancelled except for un-common acoustic path within the deep thin layer. Furthermore, quantity of traveltime difference itself is free from error in absolute positioning of kGPS. Only relative positioning error within a time of traveltime difference, e.g., 100 msec, has take effect. Taken all of these natures together, we expect the total accuracy of the proposed new technique is about 1 cm for 100-300 m of baseline length. The advantages of this new technique are facility of installation due to unecessity in clearance of direct-path and a pair of transponders alone can describes full-3D relative motion. On the other hand the disadvantages are only campaign data like GPS/A is available (not a continuous data) and baseline length must be confined within 100-300 m to achieve practical accuracy.

In the KH15-02 cruise, September 2015, we installed three seafloor transponders at the top and bottom of a cliff at 38.171N, 143.550E, 3500 m in depth along the Japan Trench. Although the transponder does not need to be locate on a steep sloop like the direct-path technique, we kept the baseline as short as possible. To perform this, we employed the Navigable Sampling System (NSS), which can remotely control the wire-end vehicle with realtime video monitor. We have carried out GPS/A measurements to thus installed transponders just after the installation and two months later to obtain the data to evaluate the accuracy. In order to monitor the activity of this target fault, further GPS/A measurement must be repeatedly required for years.

In the presentation, we introduce the detail of how most of the error sources can be cancelled and quantitatively discuss the remaining error, which are compared with the initial survey data mentioned above.

Keywords: Acoustic Ranging, GPS/A, Back Thrust, Seafloor Geodesy

An Experiment of Real-time Water Vapor Analysis using RTKLIB with MADOCA

*Yoshinori Shoji¹, Kazutoshi Sato²

1.The Second Laboratory of Meteorological Satellite and Observation System Research Department, Meteorological Research Institute, 2.Japan Aerospace Exploration Agency

We introduce the current status of experiment of real-time water vapor analysis using Global Navigation Satellite System (GNSS), represented by GPS which is mainly conducted in the Meteorological Research Institute (MRI) of the Japan Meteorological Agency (JMA), Japan. It should be noted that we are using the real-time satellite orbit information that has been analyzed by MADOCA which has been developed by Japan Aerospace Exploration Agency (JAXA). The orbit information of MADOCA includes the correction information of GPS, GLONASS, and QZSS which are observed in the MGM-Net that is an observation network covering all around the world. So far, in the real-time analysis using the RTKLIB software with MADOCA orbit correction, good agreement with radio-sonde observations was obtained. The results clearly show enough potential of this experimental configuration to contribute to the weather forecast if some problems are solved.

Keywords: GNSS, Water vapor remote sensing

Near-Real-Time GPS PPP for Time and Frequency Transfer

*Hiroshi Takiguchi¹, Tadahiro Gotoh¹, Ryuichi Ichikawa²

1.Applied Electromagnetic Research Institute, National Institute of Information and Communications Technology, 2.Ministry of Internal Affairs and Communications

GPS carrier phase time transfer is well known as a high-precision time and frequency transfer (TFT) method. GPS-CP adopts the Precise Point Positioning (PPP) technique in geodesy. PPP technique requires the precise GPS satellite orbits and clock offsets which has provided by several IGS analysis centers. Especially, rapid products and final products are usually used for TFT purpose, but they have a latency time. Therefore, we have to wait about 17 hours in case of rapid products, about 2 weeks in case of final products, when we analyze today's data. This latency is a critical fault of PPP, because other TFT technique like GPS-P3 and TWSTFT can provide the results in almost real-time.

In recent years, IGS launched the Real-Time Service (RTS) and has started providing a GNSS orbit and clock correction (hereafter real-time products) for the purpose of the real-time PPP. The accuracy of this real-time products have been monitoring at RTS web page. The satellite orbit and clock of real-time products is less than 5 cm and about 300 ps in RMS compared to rapid products respectively. The ultra-rapid products are more accurate than real-time products, and more frequently updated than rapid products, but ultra-rapid products have not been used for TFT. The real-time products is worth than ultra-rapid products at the specific field of TFT like the time link monitoring, because the real-time products can be use in real-time. In this study, we evaluated the accuracy of GPS-PPP time transfer using real-time products.

In the evaluation, we analyzed the common time link data with the common strategy (software (c5++) and models) using rapid products and real-time products separately. We didn't evaluate the real-time products at the real-time analysis. We used the two different real-time products which are provided by the different provider. One is the IGS real-time products which is provided by the IGS RTS. The IGS real-time products have been streaming (Ntrip protocol) from the several real-time analysis centers. This time, we chose the IGS03 (Kalman filter GPS+GLONASS combination) which has been provided from BKG. We received IGS03 and RTCM3EPH (Broadcast ephemeris) by using BKG Ntrip Client, and converted to clk and sp3 format in real-time. JAXA conducts real-time PPP experiment using the L-band experimental (LEX) signal from Michibiki. In this experiment, JAXA has developed Multi-GNSS orbit and clock estimator called MADOCA (Multi-GNSS Advanced Demonstration tool for Orbit and Clock Analysis) and, are providing the precise orbit and clock of GNSS by several ways (streaming, ftp, and LEX in the future). This time, we downloaded the daily sp3 file by ftp as second real-time products (MADOCA products), and used for the evaluation analysis together with IGS real-time clk file. NICT has several time links between NICT headquarters and the branches (Advanced ICT Research Institute and LF Standard Time and Frequency Transmission Stations (Ohtakadoya-yama, Hagane-yama)). In the evaluation, we analyzed the 9 months (from February 2015) data of these GPS time links. As a result of the evaluation, we confirmed that the time difference changes that were estimated using the real-time products (both IGS and MADOCA), were in good agreement with the results of using rapid products (also TWSTFT results). The difference of the results between rapid products and each real-time products were about 100 ps (IGS) and about 200 ps (MADOCA) in RMS. These differences are small enough to detect the irregular change caused by something trouble of the time links that have been monitored regularly. Therefore, these results show that the GPS PPP using real-time products has potential to monitor the time links. In the presentation, we report this evaluation in detail, and show an analysis strategy of the time link

monitoring by the near-real-time GPS PPP.

Acknowledgements: The authors thank IGS, JAXA and c5++ developers for providing their great products.

Keywords: GPS, PPP, Time and Frequency Transfer, real-time

Design and operation of a 1.5-km laser strainmeter installed in the KAGRA underground site

*Akito Araya¹, Akiteru Takamori¹, Wataru Morii², Kouseki Miyo³, Masatake Ohashi³

1.ERI, Univ. Tokyo, 2.DPRI, Kyoto Univ., 3.ICRR, Univ. Tokyo

Laser interferometers are widely used for precise measurement such as experimental physics, engineering, and metrology. Laser strainmeters in geophysical observations are one of such applications that require high displacement resolution and long-term accuracy.

In Kamioka underground site (Gifu Prefecture in Japan), a 100-m-long laser strainmeter was constructed in 2003. It proved to be sensitive enough to detect Earth's strain in a wide range of frequencies (seismic to geodetic time scale) with high resolution ($\sim 10^{-10}$ in strain) [1-3]. However, local disturbances by groundwater affected the strain measurement at very low frequencies [4]. A scaled-up interferometer is expected to improve the strain resolution by having a longer baseline and reduce local effects by spatial averaging.

A large-scale gravitational-wave detector, KAGRA, has been constructed in the new tunnel [5]. Along the KAGRA detector, a 1.5-km baseline laser interferometer has been installed for the purpose of geophysical strain observation. The laser strainmeter is formed by an asymmetric Michelson interferometer with two retro-reflectors each of which is installed in the vacuum chamber of each end. A frequency-doubled Nd:YAG laser with wavelength of 532 nm and frequency stability of $\sim 10^{-13}$ is used as a light source. The optical path of the interferometer is kept below ~ 0.1 Pa in 400-mm-diameter vacuum tubes.

For long-term continuous observation with both KAGRA detector and the laser strainmeter, several kinds of sensors are arranged to monitor the environment along in the tunnel, and their data together with the ones from KAGRA and the strainmeter are recorded by a networked data acquisition system.

Scientific targets, design of the instrument, its construction and operation will be presented.

References

- [1] S. Takemoto et al., A 100 m laser strainmeter system installed in a 1 km deep tunnel at Kamioka, Gifu, Japan, *Journal of Geodynamics*, 38, 477-488, 2004.
- [2] S. Takemoto et al., A 100m laser strainmeter system in the Kamioka Mine, Japan, for precise observations of tidal strains, *Journal of Geodynamics*, 41, 23-29, 2006.
- [3] A. Araya et al, Analyses of far-field coseismic crustal deformation observed by a new laser distance measurement system, *Geophys. J. Int.*, 181, 127-140, 2010.
- [4] A. Araya et al., Broadband observation with laser strainmeters and a strategy for high resolution long-term strain observation based on quantum standard, *J. Geod. Soc. Japan*, 53, 81-97, 2007.
- [5] Y. Aso et al, Interferometer design of the KAGRA gravitational wave detector, *Phys. Rev. D*, 88, 043007, 2013.

Keywords: strainmeter, laser, crustal deformation, KAGRA, Kamioka, gravitational wave

A proposal to avoid a leap second

*Kozo Takahashi¹

1. None

The method is shown to avoid the leap second, which needs no special operation for almost persons.

1. Decrease of rotational angular velocity: The maximum rotational angular velocity of the earth at the origin of the earth, is expressed by the following formula, because the centrifugal force caused by the angular velocity ω_0 should be less than gravity.

(In the following, **: power)

$$r \times \omega_0^{**2} = g$$

where Radius of the earth $r = 6378100$ m

$$\text{Standard gravitational acceleration } g = 9.80665 \text{ m/s}^{**2}$$

Substituting these into the above,

$$\omega_0 = 1.2400 \times 10^{**-3} \text{ rad/sec} = 107 \text{ rad/day}$$

At this value the force balances with the gravity.

The present earth has

$$\omega_p = 7.292 \times 10^{**-5} \text{ rad/sec}$$

Where ω_0 decreases exponentially,

$$\log(\omega_p / \omega_0) = -k t \quad (1)$$

Substituting followings into the above,

$$\begin{aligned} \omega_0 / \omega_p &= 1.240 \times 10^{**-3} / 7.292 \times 10^{**-5} \\ &= 16.98 \end{aligned}$$

$$\log(\omega_0 / \omega_p) = 2.833$$

and the earth's age

$$t = 4.55 \text{ bil. years} = 1.436 \times 10^{**17} \text{ secs}$$

We get

$$\begin{aligned} k &= 1.973 \times 10^{**-17} / \text{sec} = 6.226 \times 10^{**-10} / \text{year} \\ &= 0.623 / \text{bil. year} \end{aligned}$$

In past 15 years, the leap second has been substituted five times. Where the present period is T_0 , the period T after three years is expressed as follows:

$$T - T_0 = 1 \text{ sec}$$

$$T - T_0 = 2\pi(1/\omega - 1/\omega_0) = 2\pi(\omega_0 - \omega) / (\omega \times \omega_0)$$

Substituting the following into the above,

$$\omega = \omega_0 e^{**(-kt)}$$

We get

$$2\pi / \omega \{1 - e^{**(-kt)}\} = 1 \text{ sec}$$

i.e. $\omega / 2\pi = 1 - e^{**(-kt)} = kt$

Substituting $\omega = \omega_p = 7.292 \times 10^{**-5} \text{ rad/sec} = 2301 \text{ rad/year}$

and $t = 3$ years,

we get

$$k_p = 3.869 \times 10^{**-6} / \text{year}$$

Substituting the above into (1), the present half-period of the earth is calculated as follows:

$$\log 0.5 = 0.6931 = 3.869 \times 10^{**-6} \times T_p$$

$$\begin{aligned} T_p &= 0.6931 / 3.869 \times 10^{**-6} = 1.791 \times 10^{**5} \text{ years} \\ &= 180 \text{ thousands years} \end{aligned}$$

This value contradicts with the earth's age of 4.55 bil. years, that is caused by the inappropriate

definition of the second.

The present second is defined as the 9192631770 times of one period T_0 of radiant wave from Cs, whose frequency is 9.192631770 GHz. The leap second becomes unnecessary for more than hundred years, where the one second is made longer than present one, as follows: where we make the present radiant frequency $f = 9.192631770$ GHz from Cs, $(1 + 1\text{sec}/3 \text{ years} = 1 + 1.0563 \times 10^{-8})$ times, and 9.192631673 GHz, because three years are about eighth power of ten ($3 \text{ years} = 0.9467 \times 10^8 \text{ sec}$). Then the leap second becomes unnecessary, where the last three digits of the effect numbers of ten are changed to 9192631673, then

$$9192631770/9192631673 = 1 + 1.056 \times 10^{-8}$$

and one second becomes longer 1.056×10^{-8} , namely present one second becomes longer about one second for three years.

2. Effects of the change of time unit

The basic unit, speed of light, is unchanged, where the unit of meter is changed to become shorter by 0.76×10^{-8} m, caused by the second longer by 1.056×10^{-8} sec.

Keywords: leap second, avoid leap seconds

Activities of the Asia-Oceania VLBI Group for Geodesy and Astrometry (AOV)

*Ryoji Kawabata¹, Kojin Wada¹, Yoshihiro Fukuzaki¹, Masayoshi Ishimoto¹, Takahiro Wakasugi¹

1.GSI of Japan

The Asia-Oceania VLBI Group for Geodesy and Astrometry (AOV) was established in 2014 as a subgroup of the International VLBI Service for Geodesy and Astrometry (IVS) in order to foster regional collaboration of VLBI. In 2015 six regional sessions were carried out within the AOV. Moreover, on November 19-20 2015, AOV held the first Asia-Oceania VLBI Meeting hosted by the University of Tasmania in Hobart, Australia. This is the first meeting of the AOV since its establishment. AOV members shared information on their recent activities and discussed future plan of the AOV. We talk on the recent activities of the AOV.

Keywords: VLBI

Heat flux flow in the outer core and Earth's rotational motion

*Chuichi Kakuta¹

1.none

Heat flux flow in the outer core transfers heat energy from the Earth's central part into the mantle. It contributes to motion of the compressible outer core and zonal thermal wind in the outer core. These motions relate with the Earth's rotational motion.

Keywords: boundary of the outer core, heat flux flow, variation of Earth rotation

A method for attitude control of telescopes making use of the reverse pendulum

*Hideo Hanada^{1,2}, Seiitsu Tsuruta¹, Kazuyoshi Asari¹, Hiroshi Araki^{1,2}, Ken-ichi Funazaki³, Atsushi Satoh³, Hideo Taniguchi³

1.RISE, National Astronomical Observatory, 2.SOKENDAI, 3.Iwate Univ.

National Astronomical Observatory Mizusawa has developed a telescope with the focal length of 1m and diameter of 0.1m to be set on the Moon for observation of lunar rotation. It is essential to make a much small and light one to meet the requirement from smaller rockets which is a new trend in lunar and planetary explorations in Japan. We propose a new method to control the attitude of the tube by making it to be a reverse pendulum.

A tube supported by a single point at the bottom looks unstable, but it is possible to control the attitude with high sensitivity because it tends to fall down even if it slightly deviates from the vertical. We put a tube with a conical bottom on a XY stage, and surround the top of it by a ring putting 4 pressure gauges between them (Fig. 1). If the tube deviates from the vertical direction, a force acts on the pressure gauges. Then we move the bottom of the tube horizontally until the force becomes zero, and the tube is kept to be vertical. This attitude control does not restrict the optical system of the telescope because any optical element as the horizontal reference plane like a mercury pool is not necessary, nor nothing comes in the field of view.

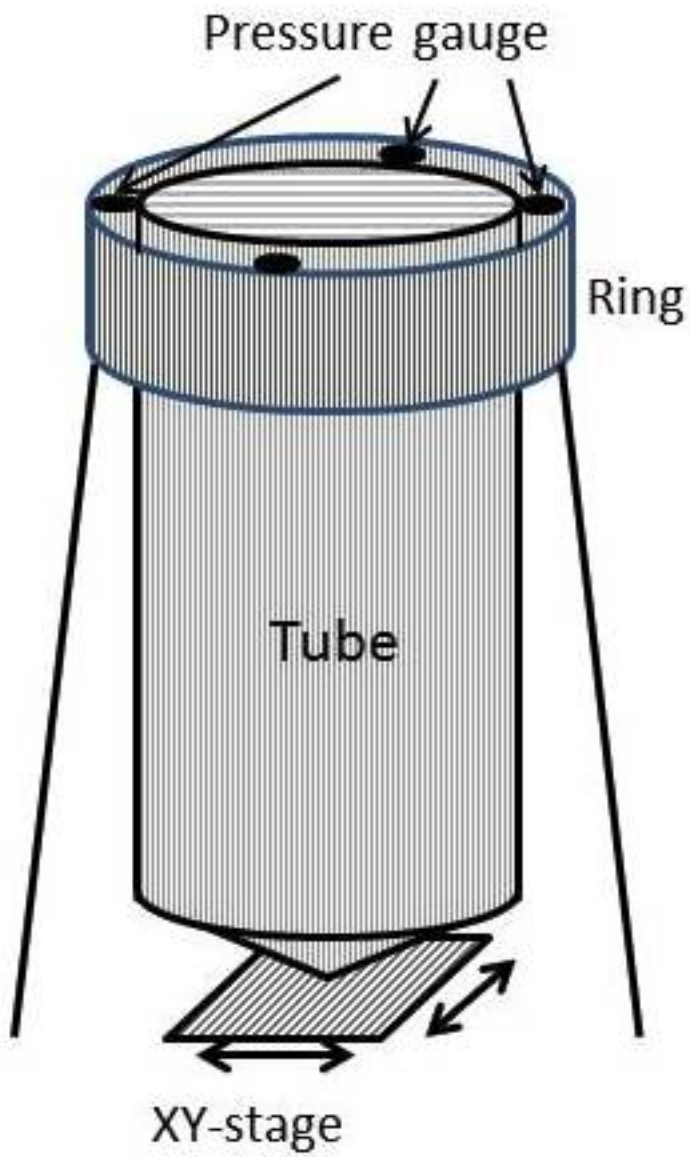
When a reverse pendulum with the mass m (kg) deviates from the vertical direction by angle θ , the force P acting horizontally is represented as $P = mg\sin\theta$. If we suppose $m = 1$ kg, $\theta = 1$ arc second (4.8×10^{-6} rad), P becomes 10^{-5} N (about $50 \mu\text{N}$). We can detect the force of 0.005mN which is about $1/10,000$ of the force in the case of 1 arc second if we use the most sensitive pressure gauge. This means that we can control the attitude of a tube with the sensitivity of 0.1 milli-arc second.

On the other hand, it has the dynamic range of 20,000 times as large as the resolution, thus the most sensitive sensor has the range of $20 \mu\text{N}$. Therefore, we must keep the tube within 20 arc seconds of the vertical direction in some other way.

As to the XY stage, it needs to have a sensitivity of 5×10^{-10} m (0.5 nm) in order to control the verticality within 1 milli-arc second. It is not impossible if we utilize a certain reduction mechanism or an inchworm.

This method can open the new way in the future mission with a small and light telescope for observation of rotation on the Moon or on the planet.

Keywords: reverse pendulum, attitude control, telescope



On a wide-band bandwidth synthesis III

*Tetsuro Kondo¹, Kazuhiro Takefuji¹

1.National Institute of Information and Communications Technology

1. Introduction

An algorithm for wideband bandwidth synthesis (WBWS) exceeding a band width of 10 GHz has been developed. The algorithm has been verified by processing actual wideband VLBI observation data. We have succeeded in a wideband bandwidth synthesis, and then the correctness of the algorithm has been confirmed. The baseline length (about 50km) is too short to investigate an ionospheric effect on a WBWS, therefore the verification of ionospheric correction has been carried out by using VLBI data simulating an ionospheric effect, and its effectiveness has been confirmed.

2. Processing algorithm

The processing algorithm is as follows.

- 1) Reference scan: define one scan observing a strong source as a reference for an inter-band delay correction and an inner-band phase correction.
- 2) Inter-band delay correction data: process each frequency band data by a conventional method and get a delay residual of each frequency band. These delay residuals are inter-band delay correction data.
- 3) Inner-band phase correction data: process each frequency band data by a conventional method and get a cross spectrum of each frequency band. These phase spectra are inner-band phase correction data.
- 4) WBWS process: combine multiple frequency bands by correcting inter-band delay using "inter-band delay correction data" and by correcting inner-band phase by using "inner-band phase correction data", and get delay residual and a wideband cross spectrum.
- 5) Ionospheric delay correction: Delta TEC (total electron content) is estimated from a wideband cross spectrum obtained by step 4). Delta TEC obtained this way is used for an ionospheric correction of correlated data of each frequency band, then step 4) is repeated to get a final result.

3. Results

WBWS software is applied to true wide-band VLBI observation data obtained by an experiment conducted on Kashima-Ishioka baseline (about 50km length) in Jan. 16, 2015. We could a good result for a wideband bandwidth synthesis. As for the ionospheric correction, the baseline length is too short to investigate the effectiveness of a correction. We, therefore, evaluated it by using data simulating an ionospheric effect on VLBI data, and we could confirm its effectiveness.

4. Summary

We have been developing an algorithm of wideband bandwidth synthesis and have established a practical algorithm. As for the verification of the ionospheric correction described here, it is not enough. We are therefore planning to verify it by using longer baseline data such as an intercontinental experiment. Lastly, the data used for WBWS are those obtained by a test experiment with GSI's Ishioka station. We would like to express our appreciation to GSI VLBI staff members for their kind support and cooperation for the experiment.

Keywords: VLBI, wideband bandwidth synthesis, ionospheric correction

VLBI application for Frequency Transfer and Development of GALA-V System (VII)

*Mamoru Sekido¹, Kazuhiro Takefuji¹, Hideki Ujihara¹, Tetsuro Kondo¹, Yuka Miyauchi¹, Masanori Tsutsumi¹, Eiji Kawai¹, Shingo Hasegawa¹, Hiroshi Takiguchi¹, Ryuichi Ichikawa², Yuko Hanado¹, Yasuhiro Koyama³, Ken-ichi Watabe⁴, Tomonari Suzuyama⁴, Jun-ichi Komuro⁵, Kenjiro Terada⁶, Kunitaka Namba⁶, Rumi Takahashi⁶, Yoshihiro Okamoto⁶, Tetsuro Aoki⁶, Takatoshi Ikeda⁷

1.National Institute of Information and Communications Technology, Space Time Standards Group, 2.Technology Policy Planning and Coordination, Global ICT Strategy Bureau Technology Policy Division, The Ministry of Internal Affairs and Communications, 3.National Institute of Information and Communications Technology, International Relations Office, 4.AIST, National Metrology Institute of Japan, Time Standards Group, 5.NICT, Outcome Promotion Department, Development support Section, 6.NICT, Outcome Promotion Department, Information System Section, 7.NICT, Network Architecture Laboratory

1. Introduction

NICT is conducting a development of the new broadband VLBI system, named GALA-V, for distant frequency comparison. By means of VLBI observations with small diameter VLBI station installed at each of atomic frequency standards to be compared, the frequency of the standard signals are compared. We have developed original broadband feed for Cassegrain type Kashima 34m antenna and enabled observation of celestial radio source in 3-14 GHz frequency range simultaneously. This broadband observation does not only improve the signal to noise ratio of VLBI observation, but also drastically improves delay measurement precision. Our GALA-V system is designed to be compatible with the VGOS (VLBI Global Observing System), which is promoted by the IVS as the next generation geodetic VLBI system, so that GALA-V and VGOS joint observation will be possible. Such collaboration with VGOS stations will be useful for GALA-V to improve the precision of frequency comparison.

2. Super broadband VLBI observation with Ishioka 13m VGOS Geodetic Station and Kashima 34m station
We have made super broadband VLBI experiment between Ishioka 13m VGOS station of GSI and NICT Kashima 34m station with broadband feed (NINJA) in 2015. Then cross correlation data of super broadband (8 GHz) were synthesized, and precise group delay observable as arrival time difference of radio signal from celestial radio source to the two VLBI stations was determined at sub-pico second (0.1 mm in light velocity) precision by one second of integration time. Although the delay measurement is in great precision, error of geodetic position determination is limited by atmospheric delay estimation error, unless many scans of observable in different direction of the sky are gathered in short time interval via fast slew antennas as required in the VGOS specification. Result of our geodetic VLBI experiment with broadband system between Ishioka 13 m and Kashima 34m stations was following to this expectation. Precision of geodetic position determination is related to measure of frequency comparison precision. Thus we need to investigate strategy to enable quick scan switching observation with the GALA-V.

3. VLBI Frequency Comparison between NMIJ and NICT.

Small diameter antenna systems of GALA-V have been installed at NICT Koganei, where Japan Standard Time (JST) is maintained, and NMIJ, where atomic time standards are developed. This NICT-NMIJ is an excellent test bed to evaluate VLBI system for frequency comparison. By using broadband observation system mentioned above, even small diameter antenna can work as a VLBI station for frequency transfer. Some experiments results with this test bed will be reported in this presentation.

4. Summary

Development of a broadband VLBI system, which is compatible with the VGOS, is being conducted in the GALA-V frequency comparison project. Broadband VLBI experiment conducted between Ishioka 13m VGOS station of GSI and NICT Kashima 34m station has demonstrated sub-pico second delay measurement in one second of integration. This is the highest precision of group delay measurement of microwave technique. NICT and NMIJ are jointly working to evaluate the VLBI application for distant frequency comparison. After verification of this technique, we will plan moving small station to foreign country to for intercontinental frequency comparison.

Acknowledgements

We wish to express our gratitude to staff of Geospatial Information Authority of Japan (GSI) for supporting our development.

Keywords: Very Long Baseline Interferometry(VLBI), VGOS(VLBI Global Observing System), Distant Frequency Comparison

Effect of adjacent frequency signal on geodetic GNSS observations

*Hiromichi Tsuji¹, Yuki Hatanaka¹, Yudai Sato¹, Tomoaki Furuya¹, Akira Suzuki¹, Hiroki Muramatsu¹, Takaaki Inukai¹, Kano Mikihara¹, Naofumi Takamatsu¹, Tomokazu Nakakuki¹, Satoshi Fujiwara¹, Tetsuro Imakiire¹, Mikio Tobita¹, Hiroshi Yara¹

1.GSI of Japan

We found a possible radio interference of 1.5 GHz LTE signals from cell-phone base stations to nearby geodetic GNSS receivers installed at 14 GEONET stations of the Geospatial Information Authority of Japan as of February 2016. At these stations, the SN ratio of observed L1 and L2 frequency GPS signals dropped suddenly on the same days when the nearby cell-phone base stations began the transmission of 1.5GHz LTE signals. The height components of GEONET final solutions (F3) of these stations are contaminated with fake periodic variations of up to 5 cm amplitudes and from 2 week to 3 month periods. There are no corresponding horizontal periodic variations. All the 14 stations are equipped with the same type of modern geodetic GNSS receivers and choke ring antennas for multi-GNSS. We suspect that the relatively high power of 1.5GHz LTE signal adjacent to L1 GPS frequency (1.57542 GHz) from the nearby cell-phone base station saturates the antenna and receiver amplifiers, and lowers the received L1 and L2 GPS signals by the receiver. However, the mechanism of the fake height variations of relatively long periods is not easy to identify. Test observations at 2 GNSS stations with notch filters provided by the receiver manufacturer to remove the 1.5 GHz LTE signal show moderate recovery of SN ratio and almost no indication of periodic height variations. The insertion of attenuator of about 5 to 10 dB has the similar effect. As interim measures, we plan to deploy optimal level attenuators to the remaining stations affected by the possible adjacent frequency channel interference.

Keywords: GNSS, adjacent frequency channel interference

Comparison of computational methods of associated Legendre functions

*Takeshi Enomoto¹

1. Disaster Prevention Research Institute, Kyoto University

Spherical harmonics composed of trigonometric and associated Legendre functions are used in geophysics and in other disciplines in science that deal with phenomena on the spherical surface. In meteorology, spherical harmonics are used to expand the prognostic variables of the atmosphere to compute the dynamical process in an atmospheric general circulation model or to analyze the energy spectrum. Recent increase in computing power allows us to use a large truncation wave number to achieve a horizontally high resolution. However, the values of associated Legendre functions of high order and degree cannot be computed accurately with the traditionally-used three-point recurrence in double precision. Alternatively, underflows can be avoided with the four-point recurrence in double precision or the three-point recurrence in extended floating arithmetic. Comparison of the two methods shows that the former and the latter have advantages in accuracy and speed, respectively. In addition, a method is shown to improve accuracy of the Fourier expansion of Legendre polynomials used along with the four-point recurrence.

Keywords: Sphere, Numerical method, Spectral method